Selective Visualization of Atoms in Extended-Chain Crystals of Oriented Poly(oxymethylene) by Atomic Force Microscopy[1]

D. Snétivy and G. J. Vancso*

Department of Chemistry, University of Toronto, 80 St. George Street, Toronto, Ontario M5S 1A1, Canada

Received December 11, 1991
Revised Manuscript Received February 21, 1992

With the invention of the scanning tunneling microscope (STM) and the atomic force microscope (AFM) imaging of materials with atomic resolution became available.[2-6] The AFM has the advantage over the STM that the sample must not be an electrical conductor. Therefore, AFM is well suited to study the micro- and nanostructure of polymeric systems.

The first AFM image of a macromolecule with molecular resolution was obtained on a polymerized monolayer of *n*-(2-aminoethyl)-10,12-tricosadinamide.[7] A detailed visualization of chain packing, quantitative values for the side-by-side interchain distances, and some structure along the chain backbone was observed. Recently, resolution of individual methylene groups and visualization of the all-trans conformation of extruded polyethylene have been achieved.[8] In this paper we report on AFM imaging of helical macromolecules in extended-chain poly(oxymethylene) (POM) crystals and selective visualization of oxygen atoms and methylene groups along the polymer backbone.

A particularly important area in polymer materials science is related to the preparation, and structure–property relationship studies of oriented solid polymers.[9] One reason for this interest is that specific mechanical properties of anisotropic polymers can significantly exceed the performance of metals. For example, the maximum measured specific Young's modulus E/ρ of uniaxially oriented polyethylene can reach 220 GPa g cm^{-3} (corresponding to a Young's modulus of ca. 210 GPa[10]), while a carbon steel AISI-SAE 1020 has an E/ρ value of 26 GPa g cm^{-3}.[11] Ultrahigh-modulus polymers are often made up of extended-chain crystals where a part of the material could still be present in chain-folded lamellae. Extended chains can be obtained in topotactic polymerization[12] or during processing, e.g., compression molding, mechanical deformation,[13] etc. The high degree of chain alignment is important to achieve maximum mechanical performance which is ultimately limited by only the strength of the chemical bonds.

POM[14] was chosen as the model material because it is the most important commercial thermoplastic that belongs to the hexagonal crystal class; hence, the number of symmetry operations which convert the crystal unit cell of POM into itself is one of the highest among polymeric materials. Oriented POM is one of the most intensively studied materials among ultrahigh-modulus polymers. Upon orientation an E value of 63 GPa (E/ρ = 45 GPa g cm^{-3}) was obtained in selective dielectric heating.[15,16] In a previous study[17] we discussed the orientation mechanism of uniaxially drawn POM and characterized the molecular orientation by X-ray pole figure measurements. This study turned our interest to a direct visualization of the chain packing by using the AFM technique.

Specimens were prepared from commercially available Ultraform H 2320 polymer (BASF). This polymer has an isotropic elastic modulus of 3.0 GPa at room temperature and an onset of melting at 164 °C, as specified by the supplier. Orientation was carried out using cylindrical samples which were obtained by extruding POM into a thermostatically controlled form. After the form was filled with the melt, it was removed from the extruder and gradually cooled down in a compression-molding press. Cylindrical specimens were uniaxially stretched in a tensile test instrument (Schenk-Trebel, Model RM-100) at a temperature of 130 °C and a stretching rate of 5 mm/min. The elastic modulus of the oriented sample in the stretched direction was 36 GPa.

DSC measurements yielded a melting point (onset of the heat flow curves) of 162 °C for the isotropic material and 169 °C for the oriented specimen. Data were obtained on a Perkin-Elmer DSC-2 operated at a heating rate of 10 °C/min. The increase in the melting point was attributed to the formation of extended-chain crystals. Further evidence for the existence of extended-chain crystals was obtained by Fourier transform infrared spectroscopy utilizing a Nicolet-FT-IR spectrometer with a beam condenser. In the oriented specimen the IR bands at 1138 and 1000 cm^{-1}, which are characteristic of folded chains,[18] are absent.

Samples for AFM studies were cleaved from stretched rods by using a Sorval MT6000 ultramicrotome with glass knives. Microtoming was carefully performed to make sure that the surfaces of the microfibrils remain intact and the sample gets cleaved only. AFM images were taken in air using a NanoScopeII instrument with an A-type scan head utilizing NanoProbe 100-μm triangular Si_3N_4 cantilevers with wide legs. The effective spring constant of the cantilever was 0.58 N m^{-1}. Images with atomic resolution were obtained in the constant-height mode.

AFM images of oriented POM on the micrometer scale showed microfibrils with a typical average diameter of 200 nm and with an axis aligned in the direction of orientation. Scans in the nanometer range were obtained on the surface of these fibrils. A typical example (raw data) is displayed in Figure 1a showing the periodic structure on the angstrom scale in two essentially perpendicular directions. Features parallel to the direction shown by the two arrows on the top and right margins were identified as images of the polymer chains. This assignment is based on values for the packing distances and on the observation that the direction of the features identified as chains coincides with the fiber direction. It is worth mentioning that upon rotation of the sample in the AFM microscope (a) both the fibers and the polymer chains become rotated to the same extent and (b) the observed chain–chain packing distances remain unchanged. In Figure 1a the nanostructure along the macromolecules is clearly visible. This feature was attributed to the visualization of individual turns of the POM helix.

An analysis of unfiltered images in the direct space and the corresponding 2D autocorrelation functions resulted in a side-by-side chain packing distance $\bar{a}$ of 4.6 ± 0.4 Å. This value agrees well with the interchain distance of 4.47 Å in the hexagonal crystal structure of POM, obtained by wide-angle X-ray diffraction (WAXD).[19-21] In the chain direction typically two different periodicities were obtained: $\bar{c}_1$ = 4.45 ± 0.3 Å and $\bar{c}_2$ = 21.0 ± 2.1 Å. This was observed also on the 2D Fourier transform of the images which typically show four "spots" in the chain direction, two on each side of the center. It is known that POM chains in the hexagonal crystal class form a 9/5 helix and have a repeat length of 17.39 Å.[19-21] The longer repeat length $\bar{c}_2$ in the chain direction was associated with the

0024-9297/92/2225-3320$03.00/0

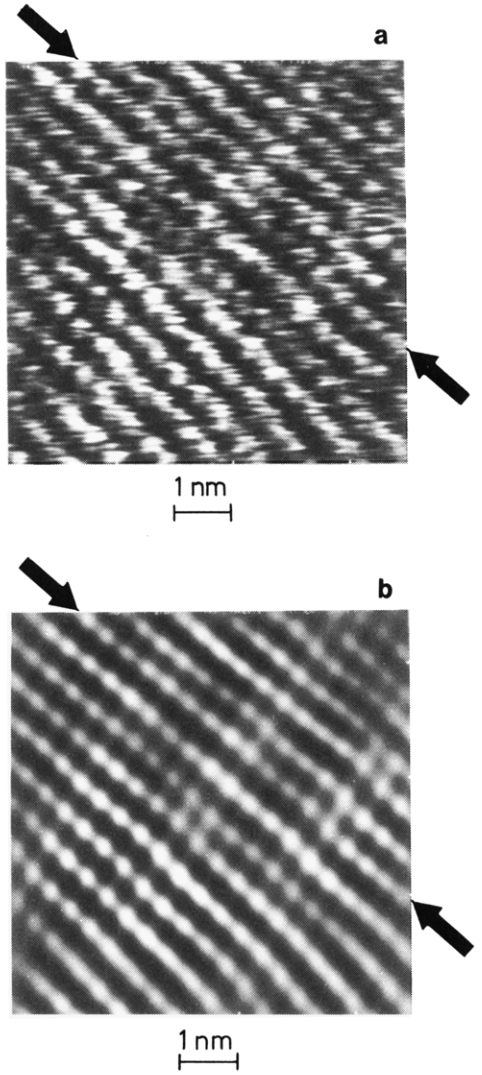

Figure 1. Atomic force microscopy image of poly(oxymethylene) with molecular resolution: (a) raw data; (b) smoothed image obtained from Fourier reconstruction. The differences in the gray tones correspond to height differences of the surface features. The image size is 7 × 7 nm.

repeat distance of the helix in the crystallographic *c* (or chain) direction. The value for $\bar{c}_2 = 21.0 \pm 2.1$ Å obtained by direct chain visualization is higher than the expected value of 17.39 Å.[19-21] The periodicity of the crystal structure for our oriented, as well as isotropic, specimens was therefore checked by WAXD experiments utilizing a Siemens D-500 instrument and a Huber texture goniometer. A shift in the reflection of the (115) crystal plane was observed in the diffractogram from $2\theta = 48.53°$ (isotropic sample) to $2\theta = 47.25°$ (uniaxially oriented sample) while the position of the (100) remained unchanged, indicating a constant value for the repeat length in the crystallographic *a* (or chain-perpendicular) direction. These results correspond to an effective stretch of the POM helix upon orientation from 17.4 (isotropic material) to 19.0 Å (stretched material). The other repeat distance $\bar{c}_1 = 4.45$ Å in the AFM images clearly corresponds to one turn of the POM helix visualized from the helix-perpendicular direction.

The filtered Fourier reconstruction of the image shown in Figure 1a is captured in Figure 1b. (No conclusions are made based on the filtered image; it solely serves the purpose of a better visualization of some details directly observed on a series of raw-data images.) The differences in the gray tones of the individual spots along the POM

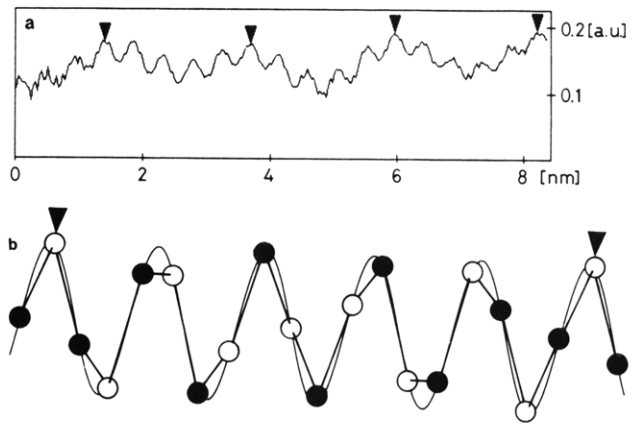

Figure 2. (a) Height profile of the macromolecule identified in Figure 1b by markers. The horizontal distance is in nanometers; the height does not scale. (b) Schematic of a POM helix. Open circles: oxygen. Filled circles: carbon. Hydrogen atoms are not shown.

helix refer to different contact force values in the vertical direction and correspond to turns of the helix with different heights, viewed from the chain-perpendicular direction. Along the chain direction two "fuzzy" turns are followed by three brighter ones, of which the middle one is the brightest. (Fuzzy and bright turns correspond to lower and higher *z*-values of the image intensities.) The height profile of the marked individual chain in Figure 1a is depicted in Figure 2a. (Parts a and b of Figure 1 display zoomed-in areas of a larger scan; the height profile in Figure 2a represents a longer chain section of the same chain which was selected before zooming-in.) For comparison, an idealized molecular helix is shown in Figure 2b. Neighboring local maxima of the measured height profile correspond to adjacent turns of the helix, while the five turns between the triangular markers represent the c repeat unit.

The visualization of the long and short nanostructure along the chain (i.e., the observation of the helix periodicity in addition to individual turns) and differences in the height values in Figure 2a suggest that the constant force contour for the AFM tip is different from the helix axis for oxygen atoms than for methylene groups. Thus, AFM is capable of differentiating between various atoms (or groups of atoms). This selective visualization of O atoms and methylene groups is attributed to the different electron contour densities of the imaged moieties. According to a least-squares refinement of the molecular structure, methylene groups possess lower electron contour densities on the cylindrical surface around the axis of POM helices than oxygen atoms.[22] Thus, while the molecular helix is imaged from the helix-perpendicular direction, the contact forces of interaction between the tip and the surface atoms will depend on the relative position of the tip to the O atoms and methylene groups. This means that atom-selective imaging can be achieved by AFM due to the sensitivity of the contact forces to the electron contour densities of the surface atoms. At this point identification of the methylene groups and oxygen atoms is not possible since the effect of higher electron contour densities on the contact force cannot be predicted. It is worth mentioning that we have recently performed AFM imaging of POM obtained from trioxane in topotactic polymerization[12] and observed "selective visualization" in a series of preliminary experiments.

Packing analyses showed that POM helices are very tightly interlocked in crystals.[23] Thus, in crystalline domains all helices are single-handed, and there is a long-

range correlation between helices in the chain-perpendicular direction. This long-range correlation can be clearly observed in the images displayed in parts a and b of Figure 1. It is interesting to mention that the 2D Fourier transforms of the unfiltered images show larger variance for the chain–chain correlation than for the periodicities along the chain. We believe that the observed large variance in the interchain packing distance is a result of imperfections in the chain packing.

Acknowledgment. Financial support by the Ontario Centre for Materials Research is gratefully acknowledged. We thank BASF AG for donation of the sample material, Dr. Brian White for his comments on the manuscript, and the Swiss Federal Institute of Technology (ETH, Zurich, Switzerland) for use of the tensile test instrument and the X-ray diffractometer.

References and Notes

(1) This paper is the second in a series dealing with atomic force microscopy of polymer single crystals.
(2) Binning, G.; Rohrer, H. *Rev. Mod. Phys.* **1987**, *59*, 615.
(3) Wickramasinghe, H. K. *Sci. Am.* **1989**, *261*, 98.
(4) Binning, G.; Quate, C. F.; Gerber, Ch. *Phys. Rev. Lett.* **1986**, *56*, 930.
(5) Hansma, P. K.; Elings, V. B.; Marti, O.; Bracker, C. E. *Science* **1988**, *242*, 209.
(6) Rugar, D.; Hansma, P. *Phys. Today* **1990**, *43*, 23.
(7) Marti, O.; Ribi, H. O.; Drake, B.; Albrecht, T. R.; Quate, C. F.; Hansma, P. K. *Science* **1988**, *239*, 50.
(8) Magonov, S. N.; Quarnstrom, K.; Elings, V.; Cantow, H.-J. *Polym. Bull.* **1991**, *25*, 689.
(9) For reference, see e.g.: Ward, I. M., Ed. *Structure and Properties of Oriented Polymers*; Applied Science Publishers: London, 1975.
(10) Ogita, T.; Yamamoto, R.; Suzuki, N.; Ozaki, F.; Matsuo, M. *Polymer* **1991**, *32*, 822.
(11) *CRC Handbook of Chemistry and Physics*, 64th ed.; CRC Press: Boca Raton, FL, 1984; p D-186.
(12) Schulz, J. *Polymer Materials Science*; Prentice-Hall: Englewood Cliffs, NJ, 1974; Chapter 2.12.
(13) Droescher, M.; Hertwig, K.; Reimann, H.; Wegner, G. *Makromol. Chem.* **1976**, *177*, 1695.
(14) It is interesting to mention that POM was the subject of Hermann Staudinger's early investigations in the 1920s at the ETH in Zurich which eventually led to the birth of polymer science. See, e.g.: Staudinger, H.; Luethy, M. *Helv. Chim. Acta* **1925**, *8*, 41.
(15) Clark, E. S.; Scott, L. S. *Polym. Eng. Sci.* **1974**, *14*, 682.
(16) Nakagawa, K.; Konaka, T.; Yamakawa, S. *Polymer* **1985**, *26*, 84; **1985**, *26*, 462.
(17) Schweizer, T.; Vancso, G. J. *Angew. Makromol. Chem.* **1989**, *173*, 85.
(18) Tanabe, Y.; Shimomura, M. *Macromolecules* **1990**, *23*, 5031.
(19) Sauter, E. Z. *Phys. Chem.* **1933**, *21B*, 186.
(20) Carazzolo, G. A. *J. Polym. Sci. A* **1963**, *1*, 1573.
(21) Uchida, T.; Tadokoro, H. *J. Polym. Sci. Polym. Phys. Ed.* **1967**, *5*, 63.
(22) Takahashi, Y.; Tadokoro, H. *J. Polym. Sci., Polym. Phys. Ed.* **1979**, *17*, 123.
(23) Geil, P. H. *Polymer Single Crystals*; Interscience: New York, 1963.